Journal of ELECTRONIC MATERIALS, Vol. 44, No. 10, 2015
DOI: 10.1007/s11664-015-3905-3

Effect of Eu Doping on the Structural, Electrical, and Dielectric Properties of $K_{0.5}Na_{0.5}NbO_3$ Ceramics for High-Temperature Capacitor Applications

LI-HUA ZHANG,[1,2,3,4] SHU-LIN WANG,[1] and FANG-HUA LIU[2]

1.—School of Mechanical Engineering, Jiangsu University, Zhenjiang, Jiangsu 212013, China. 2.—School of Mechanical Engineering, Jiangsu University of Science and Technology, Zhenjiang, Jiangsu 212003, China. 3.—e-mail: zhanglihua@just.edu.cn. 4.—e-mail: zhanglihua2000@126.com

The structural and dielectric properties of Eu-doped $K_{0.5}Na_{0.5}NbO_3$ (KNN) ceramics were investigated as a potential candidate for use in high-temperature capacitors with working temperature beyond 200°C. x-Ray diffraction results showed that tetragonal and cubic structure distortions occurred for low- and high-concentration doping, respectively. With increase of Eu content, the dielectric anomaly of the tetragonal–cubic transition was depressed and shifted to low temperature, while the temperature of the orthorhombic–tetragonal transition remained unchanged. A dielectric relaxation associated with oxygen vacancies was detected in the paraelectric phase region. The activation energy of oxygen vacancies depended on the Eu concentration and the defect compensation mechanism. KNN doped with 3 mol% Eu (KNN3Eu) showed good dielectric temperature stability (±10%) with relatively high permittivity (>1800 at 225°C) over the temperature range from 119°C to 495°C, representing a good starting point for development of high-temperature capacitor materials.

Key words: Potassium sodium niobate, dielectric properties, defects, capacitor

INTRODUCTION

Capacitors are indispensable components in modern electronic devices with important functions such as filtering, snubbing, pulse discharge, voltage smoothing, direct-current (dc) blocking, and power conditioning. However, the requirements on capacitor materials demanded by industry are increasing, with increasing demands on performance. High-temperature electronics are of particular interest for control units that can be used close to hot components, being strongly desired in the defense, aerospace, and automotive technology fields.[1] In such applications, electric components usually operate under strict conditions but must maintain good electrical properties and provide high reliability at temperatures beyond 200°C. Doping of $BaTiO_3$ or $BaTiO_3$ solid solutions often results in a broadened dielectric peak while maintaining high relative permittivity, as required, e.g., by Electronic Industry Alliance X7R specifications (temperature coefficient of capacitance within the range of ±15% between −55°C and +125°C). However, the sharp decrease in dielectric permittivity above 200°C effectively limits the usefulness of these materials at elevated temperatures.[2] Therefore, new materials with temperature-stable characteristics and high relative permittivity are needed for high-temperature applications.

Among lead-free systems, Bridger et al.[3] reported that $0.9Bi_{0.5}Na_{0.5}TiO_3$–$0.1KTaO_3$ exhibited relatively flat permittivity from 80°C to 260°C. Lim et al.[4] showed that $BiScO_3$–$BaTiO_3$–$Bi_{0.5}K_{0.5}TiO_3$ displayed good electrical properties over a wide temperature range. Materials with higher amounts of $K_{0.5}Na_{0.5}NbO_3$ (KNN) were found to exhibit high electrostrictive constants and temperature-insensi-

(Received February 5, 2015; accepted June 15, 2015; published online June 30, 2015)

tive field-induced strain, being attractive for use in high-precision positioning devices and other actuators.[5–7] The above-mentioned compositions include more than six elements, making it difficult to control the compositional homogeneity of these ceramics in commercial production. With regard to potential applications, it is vital to incorporate fewer than four kinds of raw material with reasonable price.

We present the structural and dielectric properties of rare earth Eu-doped KNN ceramics. The influence of Eu on the structure, permittivity, and loss factor of KNN was investigated. To reveal the origin of the giant dielectric loss and conductivity at high temperatures, impedance spectroscopy was carried out from 400°C to 600°C. We demonstrate that KNN doped with 3 mol% Eu is a promising dielectric for use in high-temperature applications owing to its high dielectric permittivity over a broad operational temperature range.

EXPERIMENTAL PROCEDURES

KNN ceramics doped with 0.0 mol%, 0.5 mol%, 1 mol%, 3 mol%, and 5 mol% Eu (denoted KNN0Eu, KNN0.5Eu, KNN1Eu, KNN3Eu, and KNN5Eu, respectively) were produced via a mixed oxide route using reagent-grade oxides and carbonates. First, analytical reagents (Sinopharm Chemical Reagent Co., Ltd., China) Eu_2O_3 (99.99%), Na_2CO_3 (99.5%), K_2CO_3 (99.9%), and Nb_2O_5 (99.95%) were mixed according to the stoichiometric formula and ball-milled in a planetary ball mill for 8 h at 350 rpm using zirconia balls in ethanol. After drying at 100°C, the mixed powder was calcined at 850°C for 4 h, and subsequently ball-milled again for 8 h. After drying, polyvinyl alcohol solution (PVA, 5 wt.%) was added to the powder as a binder. Pellets of 12 mm diameter and about 2 mm thickness were prepared under pressure of 80 MPa by uniaxial pressing. Samples were sintered at 1110°C to 1150°C for 4 h in an Al_2O_3 crucible at atmospheric pressure, sealed with powder of the same composition to minimize loss of volatile elements. Finally, the sintered pellets were ground and polished for measurement.

x-Ray diffraction (XRD) patterns of samples were obtained using an x-ray diffractometer (PANalytical X'Pert PRO) with Cu K_α radiation (1.54059 Å, step: 0.02°). Silver electrodes were coated on both surfaces of samples and fired at 600°C for 30 min for electrical characterization. Dielectric measurements were made isothermally, achieving thermal equilibrium by leaving the furnace at the preset temperature for 30 min. Data were recorded using a computer-controlled impedance analyzer (Agilent 4294A), over a wide range of temperature (25°C to 550°C) and frequency (100 Hz to 1 MHz) with an applied voltage of 500 mV. During cooling, impedance spectra (Z' and Z'' versus frequency) were collected from 600°C to 400°C. The modulus M^* was calculated according as $M^* = M' + jM'' = \omega C_0 Z'' + j\omega C_0 Z''$, where C_0 is the geometrical capacitance.

RESULTS AND DISCUSSION

Figure 1 shows the XRD patterns of the Eu-doped KNN ceramics. All the ceramics possessed a single-phase perovskite structure with no secondary phases observed. This indicates that Eu^{3+} diffused into the KNN lattice to form a solid solution. According to Shannon's effective ionic radius,[8] Eu^{3+} (0.947 Å for CN = 6 and 1.25 Å for CN = 12) is much larger than Nb^{5+} (0.64 Å for CN = 6) but very similar to Na^+ (1.02 Å for CN = 12) and K^+ (1.33 Å for CN = 12). Considering the principle of crystal chemistry, Eu^{3+} is suitable to enter the A site, substituting Na^+ or K^+ ions to serve as a donor-type dopant. All reflections were indexed based on the pseudocubic unit cell. As shown in the enlarged XRD patterns of the ceramics in the 2θ range from 82° to 104° in Fig. 1b, KNN0.5Eu exhibited a typical orthorhombic symmetry. As x was increased, two reflections, (222) and (22$\bar{2}$), gradually broadened

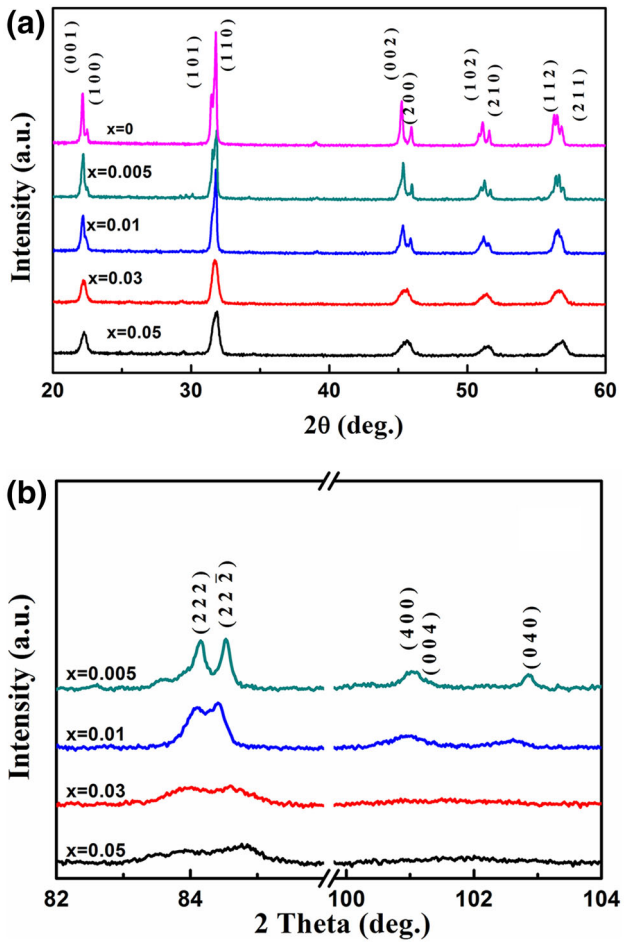

Fig. 1. (a) XRD patterns of Eu-doped KNN ceramics, indexed with pseudocubic Bragg reflection, and (b) enlargement near 100° for the pseudocubic (222) and (22$\bar{2}$) Bragg peaks.

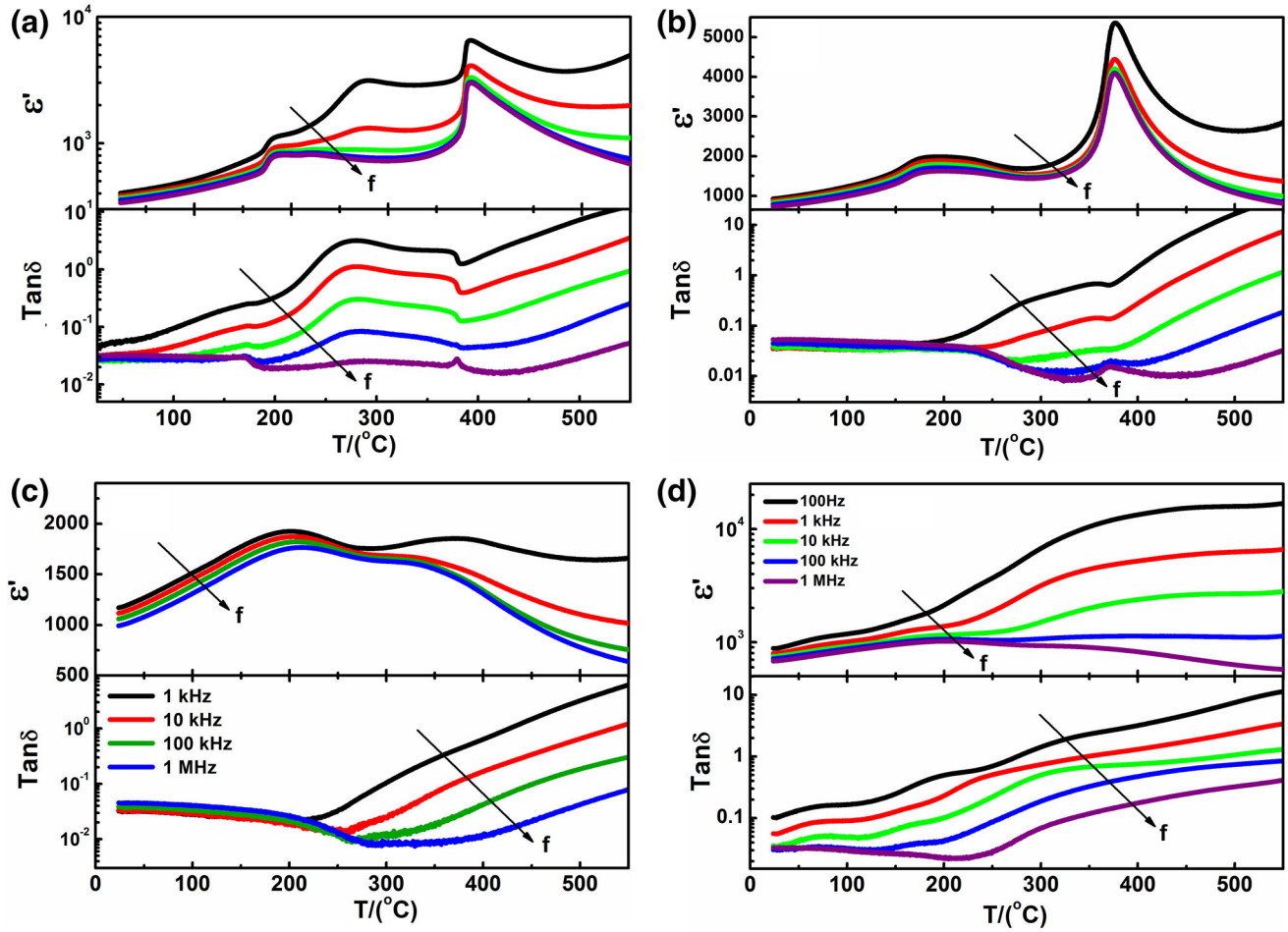

Fig. 2. Dielectric permittivity and loss factor for (a) KNN0.5Eu, (b) KNN1Eu, (c) KNN3Eu, and (d) KNN5Eu at different frequencies.

and finally combined into one peak, indicating tetragonal and cubic structure distortions at low and high Eu substitution level, respectively.

Figure 2 provides the temperature-dependent dielectric permittivity and loss factor of the Eu-doped KNN ceramics from room temperature up to 550°C. Two distinctive dielectric anomalies at high frequencies can be discerned, being common to KNN-based materials,[9] suggesting that they retained orthorhombic symmetry at room temperature. The dielectric anomaly at 200°C, known to correspond to the orthorhombic–tetragonal phase transition,[10] is independent of the Eu content, whereas the high-temperature dielectric anomaly shifted from 350°C to 400°C with increasing Eu concentration. It should be noted that a dielectric anomaly near 300°C appears at low frequencies but vanishes at high frequencies in Fig. 2a, being attributed to space-charge polarization. The two dielectric anomalies associated with phase transitions are clearly seen for KNN0.5Eu (Fig. 2a) and KNN1Eu (Fig. 2b), which are similar to pure KNN. Meanwhile, the loss factor presents two small peaks corresponding to the two phase transitions. The intensity of the low-temperature dielectric anomaly is higher than that of the high-temperature one for KNN3Eu (Fig. 2c) and KNN5Eu (Fig. 2d). Furthermore, the low-temperature dielectric anomaly exhibits frequency dispersion, being one of the distinctive features characterizing ferroelectric relaxors. Moreover, the changes in the loss factor also support the supposition that the samples have relaxor characteristic.[11] The high-temperature dielectric anomaly is depressed and shifts to low temperature. A possible reason is that the substitution of Nb^{5+} by Eu^{3+} in the KNN lattice is accompanied by the disappearance of long-range-order ferroelectric domains and the formation of nanoclusters for high concentration doping. Consequently, the orthorhombic structure suffers significant distortion with increasing Eu concentration, although the two phase transitions are still present above room temperature. This agrees with the XRD results; i.e., Eu locates at the A site for low-content doping but could enter the B site for high-content doping.

Comparison of the plots of the investigated samples clearly demonstrates that high-concentration Eu doping renders the permittivity values insensitive to temperature. Here, the temperatures of the

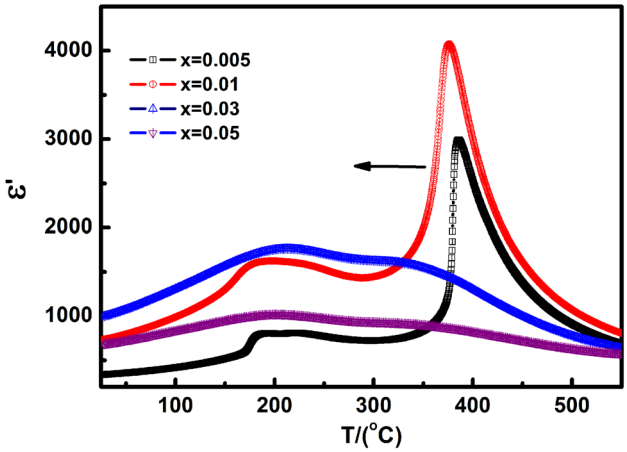

Fig. 3. Dielectric permittivity of Eu-doped KNN ceramics at 1 MHz. The temperatures of the low- and high-temperature dielectric anomalies are T_{O-T} and T_{T-C}, respectively.

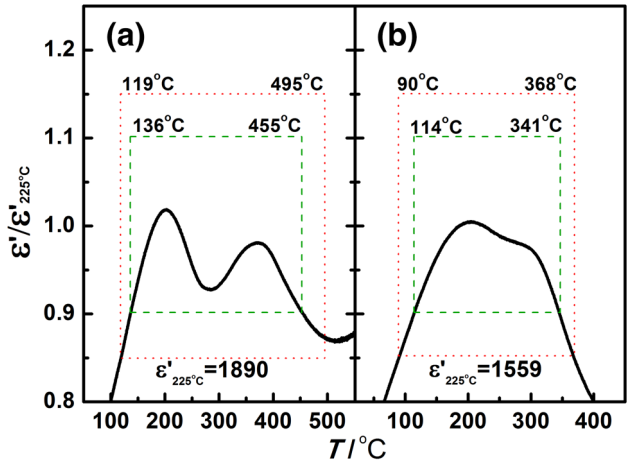

Fig. 4. Change in permittivity at 1 kHz (at 150°C) and illustration of operational range for deviation of ±10% (green dashed frame) and ±15% (red dotted frame) for (a) KNN3Eu and (b) KNN5Eu (Color figure online).

low- and high-temperature dielectric anomalies are designated as T_{O-T} (orthorhombic to tetragonal) and T_{T-C} (tetragonal to cubic). As mentioned above, T_{O-T} remained unchanged while T_{T-C} decreased with increasing Eu content, while both peaks are depressed, as shown in Fig. 3. The reduction in permittivity is responsible for the expansion of the working temperature range and for the temperature insensitivity. The feasibility of the studied materials as high-temperature dielectrics was therefore further quantified.

The permittivity normalized to the permittivity at 225°C ($\varepsilon/\varepsilon_{225°C}$) at 1 kHz is plotted in Fig. 4. Dashed and dotted frames indicate the operational ranges with ±10% and ±15% tolerance, respectively. The operational range of KNN3Eu increases from 136°C to 455°C for ±10% tolerance to 119°C to 495°C for ±15%. Unfortunately, both the dielectric permittivity and operational range decrease for KNN5Eu. The deviation in the permittivity is a notable feature since the Electronic Industries Alliance (EIA) permits ±15% deviation for commercially available X7R capacitors, which are currently designated for operation at elevated temperatures. Although limited to 125°C, the X7R material is advantageous at low temperatures down to −55°C. In contrast, the permittivity of the presented materials decreased significantly when the temperature dropped below T_{O-T}. Therefore, as an X7R capacitor, it would be beneficial to shift T_{O-T} below room temperature by chemical substitutions.

Before attempting such chemical substitutions, the defect compensation mechanism should be understood. Complex impedance spectroscopy is a powerful technique to characterize many electrical properties of a material. It is useful to evaluate the contribution of the overall electrical properties in the frequency domain due to migration of defect ions in a polycrystalline material. The variation of the normalized parameters M''/M''_{max} and Z''/Z''_{max} as a function of logarithmic frequency measured at three different temperatures is presented in Fig. 5. The peak frequencies shift towards higher frequency as one moves from Z'' to M'' for all samples at different temperatures. The magnitude of the mismatch between the Z'' and M'' peaks represents a change of the apparent polarization.[12] This difference in the peak position of the normalized parameters provides evidence of short-range conductivity.[13] Compared with KNN0.5Eu (Fig. 5a), KNN1Eu (Fig. 5b), and KNN3Eu (Fig. 5c), the curves of M''/M''_{max} and Z''/Z''_{max} for KNN5Eu (Fig. 5d) clearly illustrate that the polarization process is associated with localized conduction of multiple carriers, revealing the presence of multiple relaxation processes in the material.

The relaxation frequency (ω) at the apex of Z''/Z''_{max} (Fig. 5) is an intrinsic characteristic frequency of ceramics. The activation energies of the aforementioned dielectric response can be calculated from the relaxation time ($\omega = 1/\tau$). Relaxation frequency plotted against reciprocal temperature follows an Arrhenius law:

$$\omega = \omega_0 \exp\left[\frac{-E_H}{k_B T}\right], \quad (1)$$

where ω_0 is the preexponential factor and k_B is the Boltzmann constant. The activation energies E_H were calculated from the $\ln \omega$ versus $1/T$ data shown in Fig. 6 as 1.27(2) eV, 1.29(0) eV, 0.98(2) eV, and 0.53(5) eV for KNN0.5Eu (Fig. 6a), KNN1Eu (Fig. 6b), KNN3Eu (Fig. 6c), and KNN5Eu (Fig. 6d), respectively. The obtained activation energies are similar to literature values,[14,15] so the dielectric relaxation that occurred in this temperature range should be related to movement of ionized oxygen vacancies under the external alternating-current (ac) electric field.[16,17]

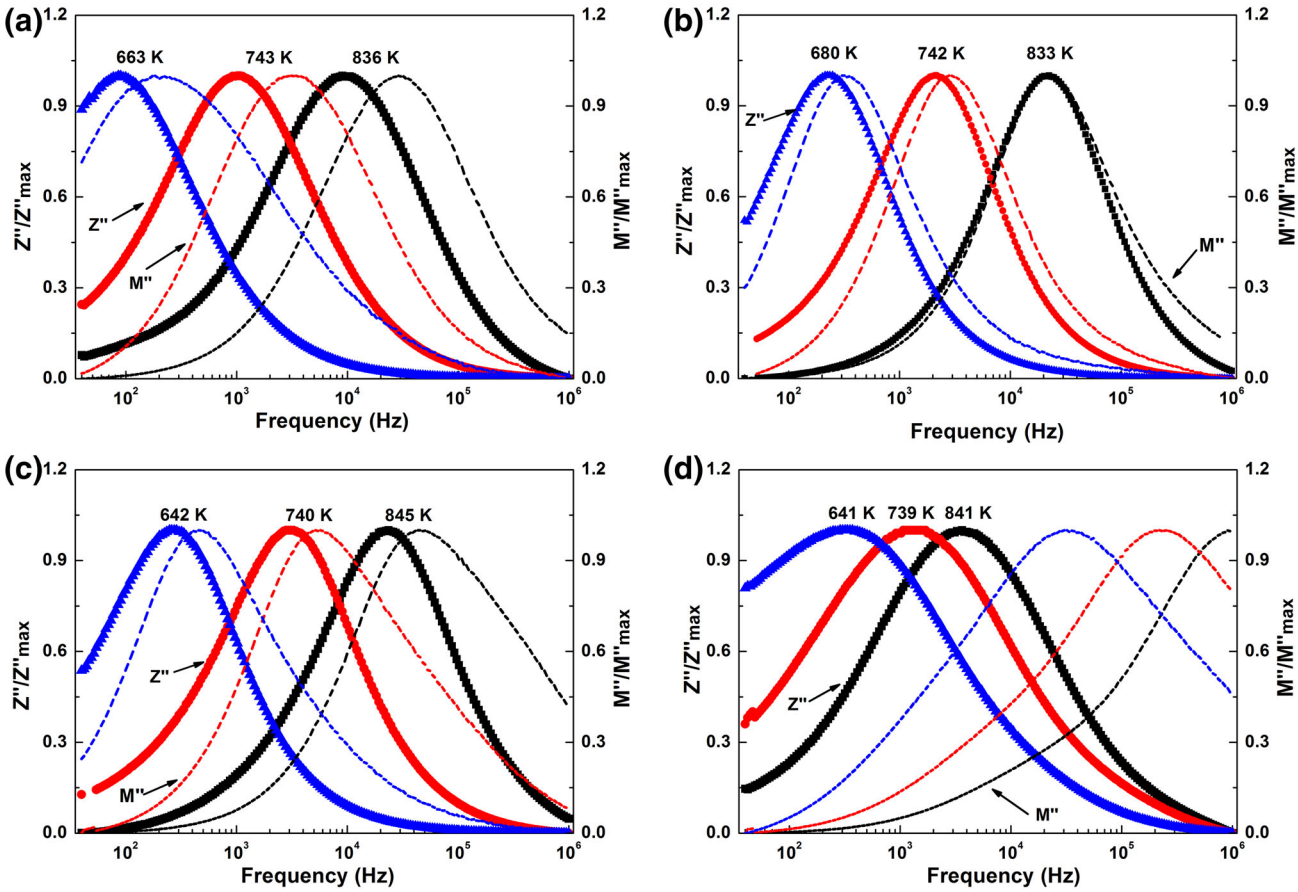

Fig. 5. Logarithmic plot of normalized parameters (M', Z') for (a) KNN0.5Eu, (b) KNN1Eu, (c) KNN3Eu, and (d) KNN5Eu at different temperatures.

Normally, dielectric materials contain a certain density of localized charges, some of which may be able to hop over many consecutive sites, ultimately giving rise to dc conductivity, while others may be restricted to shorter ranges, with the limiting case of pairs of hopping sites. The $\sigma_{ac} = \omega C_0 \varepsilon_r \tan\delta$ of all samples decreased with decreasing frequency and became independent of frequency at low frequency (not shown here). The direct-current conductivity (σ_{dc}) can be obtained by extrapolation of the low-frequency part. It is clearly described by the so-called universal dielectric response law:[18]

$$\sigma_{ac} = \sigma_{dc} + A\omega^s, \tag{2}$$

where A and s ($0 < s < 1$) are two temperature-dependent adjusting constants. Equation 2 is typical of thermally assisted tunneling between localized states. The temperature dependence of σ_{dc} thus obtained follows an Arrhenius law given by

$$\sigma_{dc} = T^{-1}\sigma_1 \exp\left[\frac{-E_{dc}}{k_B T}\right], \tag{3}$$

where σ_1 is the preexponential factor and E_{dc} is the activation energy of conductivity. E_{dc} was calculated as 1.01(1) eV, 1.09(9) eV, 0.89(8) eV, and 1.01(1) eV for KNN0.5Eu (Fig. 6a), KNN1Eu (Fig. 6b), KNN3Eu (Fig. 6c), and KNN5Eu (Fig. 6d), respectively, from the ln $T\sigma_{dc}$ versus $1/T$ plot in Fig. 6. The activation energy is similar to that reported in literature.[19–21] Consequently, the high-temperature conductivity should be associated with long-range hopping of oxygen vacancies.

Comparing the relaxation activation energy (E_H) and conductivity activation energy (E_{dc}), the former obviously depends on the Eu content, first increasing then decreasing. The value of the thermal activation energy is related to the concentration of oxygen vacancies. Na/K evaporation results in oxygen vacancies in pure KNN, which induces intrinsic oxygen vacancies as follows:[22]

$$K_2O + Na_2O = V'_K + V'_{Na} + V^{\bullet\bullet}_O + 1/2Na_2O(g) + 1/2K_2O(g) \tag{4}$$

When Eu_2O_3 is added to KNN, it tends to occupy the A site due to the similar ionic radius of Eu^{3+} and Na^+/K^+. Therefore, donor compensation (Eq. 5) could happen and thus restrain the oxygen vacancy concentration. Consequently, the activation energy

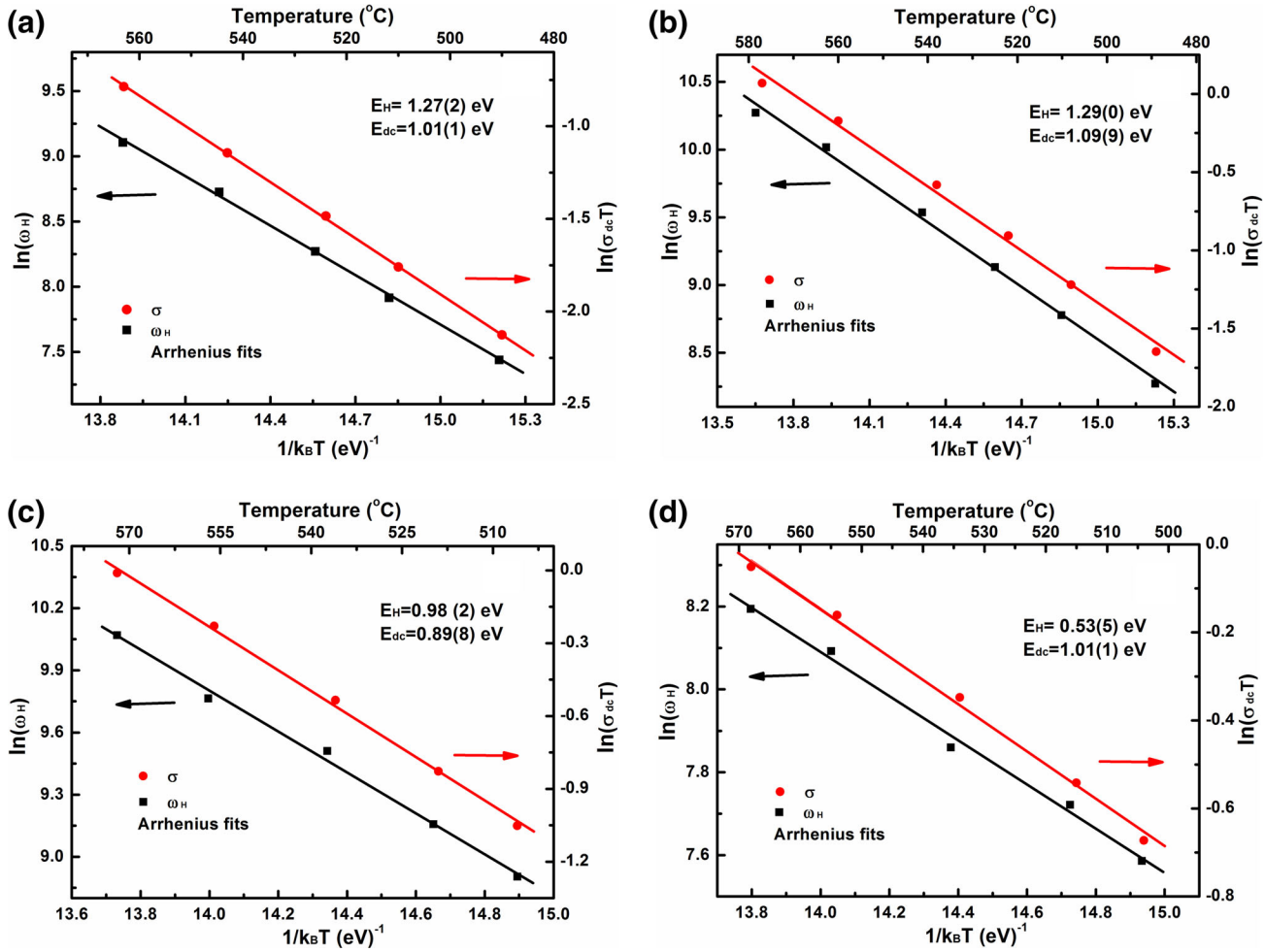

Fig. 6. Temperature dependence of the most probable relaxation frequency obtained from the normalized imaginary part of impedance plots and Arrhenius plot of dc conductivity for (a) KNN0.5Eu, (b) KNN1Eu, (c) KNN3Eu, and (d) KNN5Eu. Squares are experimental points, and solid lines are least-squares straight-line fits.

of oxygen vacancies will increase. The maximum activation energy is presented by KNN1Eu.

$$Eu_2O_3 + 2V_O^{\bullet\bullet} = 2Eu_{Na}^{\bullet\bullet} + 6O \quad (5)$$

On further increasing the content of Eu, it locates at the B site to substitute for Nb, which results in an increase of oxygen vacancies (Eq. 6).

$$Eu_2O_3 + Nb_2O_5 = 2Eu'_{Nb} + 2Nb_{Nb} + V_O^{\bullet\bullet} + 16O_O \quad (6)$$

The aforementioned compensation mechanism is in agreement with the XRD results (Fig. 1) and the temperature dependence of the dielectric permittivity (Fig. 2). Consequently, for low-concentration Eu doping, Eu enters the A site and restrains the concentration of oxygen vacancies (Fig. 6), while the dielectric anomaly of the tetragonal–cubic phase transition is not depressed (Fig. 2a and b). However, for high-level doping of Eu, it diffuses into the B site to substitute for Nb and leads to structural distortion. Additionally, the dielectric anomaly of the tetragonal–cubic phase transition is depressed (Fig. 3), which results in good dielectric temperature stability (Fig. 4). On the other hand, the concentration of oxygen vacancies will increase due to acceptor doping (Eu substitutes for Nb) (Fig. 6).

CONCLUSIONS

Rare earth Eu-doped KNN ceramic compositions for potential use in high-temperature dielectric applications were developed. The compositions provided not only high dielectric permittivity but also a wide operational temperature range. The dielectric properties of the Eu-doped KNN ceramics depend on the defect compensation mechanism; i.e., Eu enters the A site for low-concentration doping but diffuses to the B site for high-level doping. KNN3Eu is suitable for development of high-capacitance, cost-effective capacitors for high-temperature applications beyond 200°C.

ACKNOWLEDGEMENTS

The research work was supported by the National Natural Science Foundation of China (Grant No. 51275217).

REFERENCES

1. R.W. Johnson, J.L. Evans, P. Jacobsen, J.R. Thompson, and M. Christopher, *IEEE Trans. Electron. Packag. Manuf.* 27, 164 (2004).
2. N. Raengthon, T. Sebastian, D. Cumming, I.M. Reaney, and D.P. Cann, *J. Am. Ceram. Soc.* 95, 3554 (2012).
3. K. Bridger, A.V. Cooke, and W.A. Schulze, U.S. Patent No. US7,697,263 B2 (13 April 2010).
4. J.B. Lim, S.J. Zhang, N. Kim, and T.R. Shrout, *J. Am. Ceram. Soc.* 92, 679 (2009).
5. S.T. Zhang, A.B. Kounga, E. Aulbach, H. Ehrenberg, and J. Rödel, *Appl. Phys. Lett.* 91, 112906 (2007).
6. L. Liu, D. Shi, M. Knapp, H. Ehrenberg, L. Fang, and J. Chen, *J. Appl. Phys.* 116, 184104 (2014).
7. R. Dittmer, W. Jo, D. Damjanovic, and J. Rödel, *J. Appl. Phys.* 109, 034107 (2011).
8. R.D. Shannon, *Acta Cryst.* A32, 751 (1976).
9. F. Cordero, F. Craciun, F. Trequattrini, E. Mercadelli, and C. Galassi, *Phys. Rev. B* 81, 144124 (2010).
10. L. Liu, Y. Huang, Y. Li, L. Fang, H. Dammak, H. Fan, and M. Pham, *Mater. Lett.* 68, 300 (2012).
11. H. Qian and L.A. Bursill, *Int. J. Mod. Phys. B* 10, 2007 (1996).
12. R. Gerhardt, *J. Phys. Chem. Solids* 55, 1491 (1994).
13. X. Yao, Z. Chen, and L.E. Cross, *J. Appl. Phys.* 54, 3399 (1983).
14. L. Liu, H. Fan, L. Fang, X. Chen, H. Dammak, and M. Pham, *Mater. Chem. Phys.* 117, 138 (2009).
15. C. Ang, Z. Yu, and L.E. Cross, *Phys. Rev. B* 62, 228 (2000).
16. L. Liu, Y. Huang, C. Su, L. Fang, M. Wu, and C. Hu, *Appl. Phys. A* 104, 1047 (2011).
17. B.S. Kang, S.K. Choi, and C.H. Park, *J. Appl. Phys.* 94, 1904 (2003).
18. A.K. Jonscher, *J. Phys. D Appl. Phys.* 32, R57 (1999).
19. L. Liu, Y. Huang, Y. Li, M. Wu, L. Fang, C. Hu, and Y. Wang, *Phys. B* 407, 136 (2012).
20. S. Wu, W. Zhu, L. Liu, D. Shi, S. Zheng, Y. Huang, and L. Fang, *J. Electron. Mater.* 43, 1055 (2014).
21. H.S. Shulman, D. Damjanovic, and N. Setter, *J. Am. Ceram. Soc.* 83, 528 (2000).
22. L. Liu, M. Wu, Y. Huang, Z. Yang, L. Fang, and C.Z. Hu, *Mater. Chem. Phys.* 126, 769 (2011).